PEGylation Site-Dependent Structural Heterogeneity Study of MonoPEGylated Human Parathyroid Hormone Fragment hPTH(1-34)

ARTICLE *in* LANGMUIR · AUGUST 2014

Impact Factor: 4.46 · DOI: 10.1021/la501689d · Source: PubMed

9 AUTHORS, INCLUDING:

Wen-Yih Chen

National Central University

140 PUBLICATIONS **2,436** CITATIONS

Langmuir

Article

pubs.acs.org/Langmuir

PEGylation Site-Dependent Structural Heterogeneity Study of MonoPEGylated Human Parathyroid Hormone Fragment hPTH(1−34)

Chih-Ying Liu,[†,‡] Xin Li,[#] Wen-Yih Chen,[‡] Li-Chiao Chang,[§] Yi-Fan Chen,[‡] Hsin-Lung Chen,[∥] Ya-Sen Sun,[‡] Hsiu-Yun Lai,[⊥] and E-Wen Huang*[,†]

[†]Department of Materials Science & Engineering, National Chiao Tung University, Hsinchu 30010, Taiwan

[#]Biology and Soft Matter Division, Oak Ridge National Laboratory, Oak Ridge, Tennessee 37831, United States

[‡]Department of Chemical and Materials Engineering, National Central University, Jhongli, 32001, Taiwan

[§]ScinoPharm Taiwan, Limited, Tainan 74144, Taiwan

[∥]Department of Chemical Engineering, National Tsing Hua University, Hsinchu 30013, Taiwan

[⊥]Department of Family Medicine, National Taiwan University Hospital Hsin-Chu Branch, Hsinchu 30059, Taiwan

Supporting Information

ABSTRACT: The structures of C- and N-terminally monoPEGylated human parathyroid hormone fragment hPTH(1−34) as well as their unmodified counterparts, poly(ethylene glycol) (PEG) and hPTH(1−34), have been studied by small-angle neutron scattering (SANS). The scattering results show that free hPTH(1−34) in 100 mM phosphate buffer (pH 7.4) aggregates into clusters. After conjugation with PEG, the PEG−peptide conjugates self-assemble into a supramolecular core−shell structure with a cylindrical shape. The PEG chains form a shell around the hPTH(1−34) core to shield hPTH(1−34) from the solvent. The detailed structural information on the self-assembled structures is extracted from SANS using a model of the cylindrical core with a shell of Gaussian chains attached to the core surface. On the basis of the data, because of the charge−dipole interactions between the conjugated PEG chain and the peptide, the conjugated PEG chain forms a more collapsed conformation compared to free PEG. Moreover, the size of the self-assembled structures formed by the C-terminally monoPEGylated hPTH(1−34) is about 3 times larger than that of the N-terminally monoPEGylated hPTH(1−34). The different aggregation numbers of the self-assembled structures, triggered by different PEGylation sites, are reported. These size discrepancies because of different PEGylation sites could potentially affect the pharmacokinetics of the hPTH(1−34) drug.

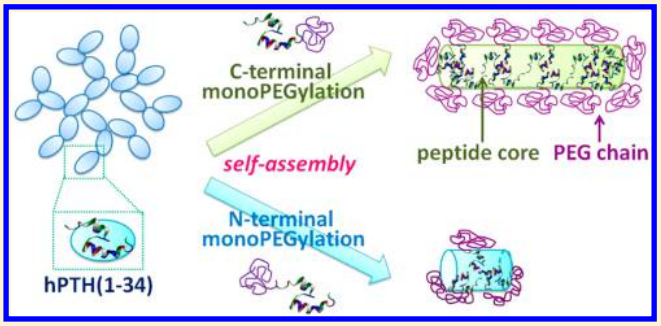

INTRODUCTION

Osteoporosis is defined as impairment of bone mass and microarchitecture that increases the incidence of fragility fracture.[1−3] The prevalence of osteoporosis influences both men and women with advanced age. Hence, osteoporosis therapy demands much more attention for the ongoing aging society. Human parathyroid hormone (hPTH), a protein with 84 amino acids and molecular weight (MW) of 9425 Da, is responsible for the calcium homeostasis and bone metabolism in our body.[4] The N-terminal 1−34 fragment of hPTH [hPTH(1−34)], also referred to as teriparatide, is the biologically active moiety that has been approved by the U.S. Food and Drug Administration (FDA) for treatment of osteoporosis for both men and women.[4] However, hPTH(1−34) is proteolytically unstable in human serum with a short circulation half-life (less than 1 h). Conjugating a poly(ethylene glycol) (PEG) chain to hPTH may shield the drug from proteolysis to prolong its circulation half-life.

Protein and peptide drugs are promising therapeutic agents. However, there are several challenges that limit their practical applications, such as low solubility, unstable subjected to temperature and pH variations, degradation by proteolytic enzymes, and rapid kidney clearance.[5] Studies have shown that covalently attaching PEG, a process known as PEGylation, provides a new path to overcome these hurdles.[6−10] The properties of these hybrid conjugates depend upon the conformation of polypeptide and conjugated PEG.[11] Therefore, it is important to systematically investigate the conformation of PEG−polypeptide conjugates and the interactions between them for structure−activity considerations. The detailed structural analyses are important for development of "bio-betters".

Received: May 3, 2014
Revised: July 19, 2014
Published: August 28, 2014

There are several studies that have investigated the structure of PEGylated protein-based conjugates using small-angle scattering.[12,13] Pai et al.[12] pioneered small-angle neutron scattering to study the conformation of monoPEGylated lysozyme and monoPEGylated human growth hormone. They reported that the PEG−protein conjugate had a dumbbell conformation, with the PEG chain adopting a random coil adjacent to the globular protein.[12] Svergun et al.[13] studied the solution structure of hemoglobin (Hb), which was conjugated with two or six to seven PEG chains. The PEGylation process does not compromise the tertiary structure of Hb. The reconstructed low-resolution structures show that part of the conjugated PEG chain occupies the cavities between Hb subunits, while the rest of PEG protrudes away from the Hb surface.[13]

In comparison to the well-defined and more rigid structures of proteins, peptides are more flexible and their structures are more easily affected by the conjugated PEG chains as well as the surrounding medium. Despite the development of PEG−peptide conjugates with pharmaceutical purposes, their structures are very difficult to resolve. The structural change induced by PEGylation could play an important role in the pharmacokinetics of the PEG−peptide drugs. For example, the peptides studied by Shu et al.[11,14] and Lund et al.[15] were specially designed to form 3-helix (1CW) or 4-helix (H10H24) bundles. After PEGylation, the peptide part of the resulting side conjugates still formed 3-helix (1CW−PEG) or 4-helix (H10H24−PEG) bundles. On the basis of several of the aforementioned successful studies on the structures of PEGylated peptides by small-angle scattering examining designated peptides as a model peptide, we investigate commercial products from ScinoPharm Taiwan, Ltd.

Specifically, small-angle neutron scattering (SANS) is used to investigate the structure of hPTH(1−34) and monoPEGylated hPTH(1−34) at two different PEGylation sites: C terminus and N terminus. The structure that is formed by the particles of hPTH(1−34) undergoes a dramatic change because of monoPEGylation. We focus on the (1) size discrepancy of the self-assembled structures, which is triggered by different PEGylation sites, and (2) conformational difference between the free PEG chain and the conjugated PEG chain.

EXPERIMENTAL SECTION

Materials. Recombinant human parathyroid hormone (1−34) [hPTH(1−34), SVSEIQLMHNLGKHLNSMERVEWLRKKLQDVHNF, MW = 4.1 kDa, >95%], C-terminally monoPEGylated hPTH(1−34) (Cterm-PEG−PTH(1−34), MW = 9.1 kDa, >95%), and N-terminally monoPEGylated hPTH(1−34) (Nterm-PEG−PTH(1−34), MW = 9.1 kDa, >95%) with site specificity of 100% were obtained from ScinoPharm (Taiwan). Methoxy poly(ethylene) glycol (MPEG, average M_n = 5 kDa) was purchased from Sigma-Aldrich (St. Louis, MO). Deuterium oxide (D_2O, D > 99%) was purchased from Cambridge Isotopes (Tewksbury, MA). PEG, hPTH(1−34), and Cterm-PEG−PTH(1−34) were dissolved in 100 mM phosphate buffer (pH 7.4) at a concentration of 4 mg/mL.

SANS. SANS measurements of free PEG chain and hPTH(1−34) were performed at the CG3 beamline (Bio-SANS) of the High Flux Isotope Reactor (HFIR) in Oak Ridge National Laboratory (ORNL), Oak Ridge, TN. Two sample−detector distances, 0.3 and 6 m, were used to provide the q range from 0.007 to 0.4 Å^{-1} ($q = 4\pi \sin(\theta)/\lambda$, where 2θ is the scattering angle and λ is the wavelength). The exposure time was 15 and 30 min for sample−detector distances of 0.3 and 6 m, respectively. The SANS experiments for Cterm-PEG−PTH(1−34) and Nterm-PEG−PTH(1−34) were performed at the BL6 beamline (EQ-SANS) of the Spallation Neutron Source (SNS) in ORNL. The sample−detector distances were 2.5 and 5 m, covering the q range from 0.006 to 0.4 Å^{-1}. The exposure times for the sample−detector distances of 2.5 and 5 m were 0.5 and 2 h, respectively. All of the samples were held in 5 mm path length Banjo cells and measured under three different temperatures of 25, 37, and 55 °C.

Data Analysis. The two-dimensional (2D) scattering patterns were radially averaged to obtain one-dimensional (1D) scattering profiles. The radius of gyration, R_g, was calculated by Guinier analysis.[16] At the Guinier regime ($qR_g < 1$), the scattering profile is model-independent and given by the expression[16]

$$\ln[I(q)] = \ln[I(0)] - \frac{q^2 R_g^{\,2}}{3} \quad (1)$$

where $I(0)$ is the extrapolated intensity at zero scattering angle (forward scattering). The exponent decay of the scattering profiles were analyzed by power law analysis.[17] To extract the structural information on the samples, the experimental scattering profiles were fitted by the program Igor Pro with the package developed by the National Institute of Standards and Technology (NIST) Center for Neutron Research (NCNR package) and the software package SASfit developed by the Paul Scherrer Institute (PSI).[18,19]

RESULTS AND DISCUSSION

hPTH(1−34). Figure 1 shows the SANS profile of 4 mg/mL hPTH(1−34) in 100 mM phosphate buffer at 25, 37, and 55 °C. The scattering profiles show two distinct structural levels. The level above 0.045 Å^{-1} corresponds to the scattering contribution from primary particles. The upturn at the low q region suggests that the primary particles aggregate in phosphate buffer.[20]

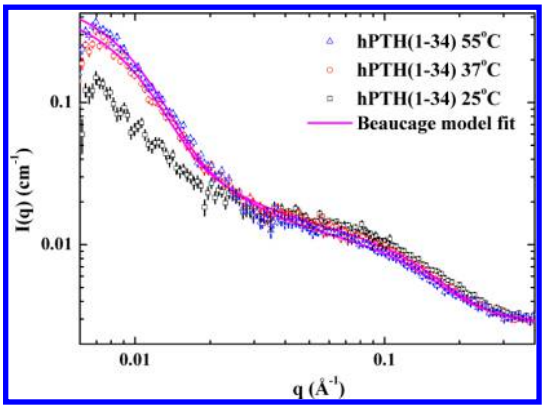

Figure 1. SANS profiles of hPTH(1−34) in phosphate buffer at (□) 25 °C, (○) 37 °C, and (△) 55 °C. The fitting method is the Beaucage model with two levels.

The SANS profiles of hPTH(1−34) were first analyzed by power law.[17] The results of power law analysis of hPTH(1−34) SANS profiles are tabulated in Table 1. In the q range from 0.1 to 0.25 Å^{-1}, the scattering intensity decays with approximately $I \sim q^{-1}$. This indicates that the primary particle has an extended shape, such as cylinder and ellipsoid. We reconstructed the solution structure of hPTH(1−34) determined by nuclear magnetic resonance (NMR).[21] The surface structure of hPTH(1−34), which was visualized by the program PyMOL[22] revealed a triaxial ellipsoid (see the Supporting Information). The detailed structural information on the ellipsoidal primary particle was extracted by fitting the SANS profiles from the higher q region with a triaxial ellipsoid form factor.[23]

dx.doi.org/10.1021/la501689d | Langmuir 2014, 30, 11421−11427

Table 1. Structure Parameters of hPTH(1−34) in Phosphate Buffer at 25, 37, and 55 °C

			semi-axes		
temperature (°C)	$R_{g\ aggregate}$ (Å)	$R_{g\ primary}$ (Å)	a (smallest) (Å)	b (Å)	c (largest) (Å)
25			7.5 ± 3.1	11.9 ± 2.6	24.5 ± 1.3
37	200.1 ± 3.5	12.7 ± 0.2	8.8 ± 2.8	12.7 ± 2.7	23.4 ± 1.0
55	194.2 ± 2.9	12.9 ± 0.3	7.7 ± 3.5	13.1 ± 2.8	26.6 ± 1.7

To extract the radii of gyration, R_g, of the aggregate and primary particle, the Beaucage model with two levels was used to fit the SANS profiles of hPTH(1−34). The fitting function is[24]

$$I(q) = G_i e^{-q^2 R_{g\,i}{}^2/3} + B_i \left\{ \frac{\left[\mathrm{erf}\left(\frac{-qR_{g\,\mathrm{aggregate}}}{\sqrt{6}} \right) \right]}{q^{P_i}} \right\}^{P_i} + \mathrm{Bkg} \quad (2)$$

where G_i is the exponent prefactor, B_i is a constant prefactor for the power law term, and Bkg is the incoherent background. Because of the lack of Guinier region for the SANS profile at 25 °C, the precise aggregate size cannot be obtained from our data. The SANS scattering profiles of hPTH(1−34) at 37 and 55 °C and the fitted curves by the Beaucage model with two levels are shown in Figure 1. The fitting results are listed in Table 1. The size of the primary particle has no obvious temperature dependence. However, the size of the aggregate decreases with increasing the temperature. Because the aggregate is held together by the hydrophobic interactions between peptides, the temperature dependence of the aggregate size could be attributed to the change in hydrophobicity of hPTH(1−34).[25] As the temperature increases, the hydrophobicity of hPTH(1−34) would increase, causing the primary particles to pack more compactly together, and lead to a smaller aggregate size.

To extract the three semi-axes of the ellipsoidal primary particle, the triaxial ellipsoid form factor was used to fit the high q region of the SANS profiles of hPTH(1−34). This form factor calculates a triaxial ellipsoid with uniform scattering length density, which is averaged over all possible orientations.[23] Because the scattering profiles of hPTH(1−34) contained the contribution for both the aggregate and primary particle, we subtracted the scattering contribution from the aggregate before fitting the data with the triaxial ellipsoid form factor. The SANS scattering profiles of the primary particle and the fitted curves are shown in Figure 2. The three semi-axes of the primary particle obtained from model fitting are listed in Table 1. There is only a slight temperature dependence of the ellipsoidal primary particle.

The number of hPTH(1−34) forming one primary particle can be obtained by calculating the molecular mass of a primary particle using eq 3

$$\frac{\mathrm{MW}_{\mathrm{primary}}}{\mathrm{MW}_{\mathrm{standard}}} = \frac{I(0)_{\mathrm{primary}}}{I(0)_{\mathrm{standard}}} \quad (3)$$

where $\mathrm{MW}_{\mathrm{primary}}$ and $\mathrm{MW}_{\mathrm{standard}}$ are the molecular weights of the primary particle and standard, respectively. $I(0)$ is the intensity at zero scattering angle. Here, we used lysozyme (MW = 14.3 kDa) as the standard. The MW of a primary particle was calculated as 3811 Da. Because the MW of hPTH(1−34) is 4117 Da, it is estimated that each primary particle contains one hPTH(1−34).

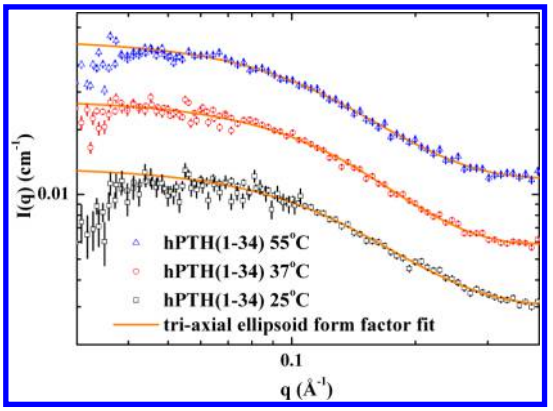

Figure 2. SANS profiles of the hPTH(1−34) primary particle in phosphate buffer at (□) 25 °C, (○) 37 °C, and (△) 55 °C and the fitted curves by the triaxial ellipsoid form factor. The SANS profiles and the fitted curves at 37 and 55 °C have been shifted vertically for clarity.

Cterm-PEG−PTH(1−34) and Nterm-PEG−PTH(1−34). Figure 3 shows the SANS profiles of hPTH(1−34) primary particles (without the contribution from the peptide aggregates), Cterm-PEG−PTH(1−34) and Nterm-PEG−PTH(1−34). The intensities at zero scattering angle, $I(0)$, of Cterm-PEG−PTH(1−34) and Nterm-PEG−PTH(1−34) are much larger than that of the hPTH(1−34) primary particle [$I(0)_{\mathrm{Cterm}}$ = 0.29 cm^{-1}, $I(0)_{\mathrm{Nterm}}$ = 0.04 cm^{-1}, and $I(0)_{\mathrm{hPTH(1-34)}}$ = 0.01 cm^{-1}]. Besides, the Guinier regions of Cterm-PEG−PTH(1−34) and Nterm-PEG−PTH(1−34) have shifted to a much lower q region compared to that of the hPTH(1−34) primary particle. These indicate that the structures formed by Cterm-PEG−PTH(1−34) and Nterm-PEG−PTH(1−34) are larger than that of the hPTH(1−34) primary particles. The size difference could be attributed to one of the two reasons: (1) the peptide or conjugated PEG chain extends to occupy a larger

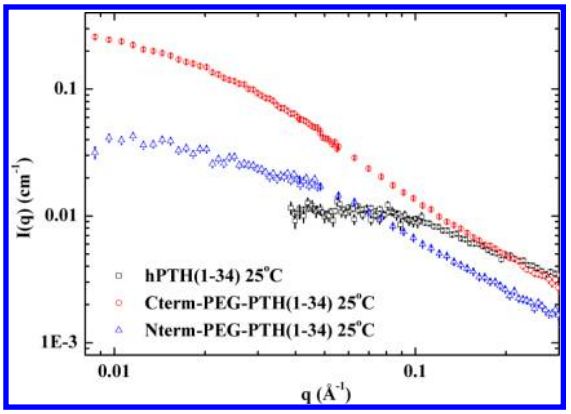

Figure 3. SANS profiles of hPTH(1−34) primary particles (without the contribution from the peptide aggregates), Cterm-PEG−PTH(1−34) and Nterm-PEG−PTH(1−34).

dx.doi.org/10.1021/la501689d | Langmuir 2014, 30, 11421−11427

volume, or (2) the PEG−peptide conjugates self-assemble into a supermolecular structure. Because PEG is more hydrophilic than hPTH(1−34) and it is unlikely that hydrophobic hPTH(1−34) would extend in the solvent, it is expected that, after conjugating PEG to hPTH(1−34), the conjugates would self-assemble into a supermolecular structure. The PEG chains of the conjugates would form a shell around the peptide core to reduce its solvent-accessible surface area.

We used the form factor of a micelle model with a cylindrical core and Gaussian polymer chains attached to the surface developed by Pedersen and Gerstenberg to fit the SANS profiles of Cterm-PEG−PTH(1−34) and Nterm-PEG−PTH(1−34).[26,27] In some small-angle scattering studies, the micelles have been assumed to be centrosymmetric, where the corona has a radial or constant scattering length density profile.[26,28−30] (e.g., the cap-and-gown model developed by Liu et al.[29] and the form factor of a core−shell cylinder developed by Livsey et al.[30]) However, the centrosymmetry models fail to describe the "blob scattering" at a high q region, which originates from the chains in the corona.[26] Different from centrosymmetry models, the form factor developed by Pedersen and Gerstenberg describes the corona as consisting of non-interacting Gaussian chains and assumes a mushroom polymer conformation.[26]

The form factor is shown in Figure 4, where N_{agg} is the aggregation number of the micelle and β_{core} and β_{brush} are the

$$I = N_{agg}^2\beta_{core}^2P_{core}(q) + N_{agg}\beta_{brush}^2P_{brush}(q) + 2N_{agg}^2\beta_{core}\beta_{brush}S_{core-brush}(q)$$
$$+N_{agg}(N_{agg}-1)\beta_{brush}^2S_{brush-brush}(q)$$

Figure 4. Form factor of a micelle model with a cylindrical core and Gaussian polymer chains attached to the surface developed by Pedersen and Gerstenberg.[33,40]

total excess scattering length of a block in the core and corona, respectively. P_{core} represents the form factor for a monodispersed, right circular cylinder core that is taken all possible orientations into account.[31] The self-correlation term of the brush, P_{brush}, describes the polymer chains in the corona to be Gaussian coils using the Debye function.[32] $S_{core-brush}$ describes the cross-term between the core and chains, while $S_{brush-brush}$ describes the cross-term between different polymer chains.[33]

The SANS profiles of Cterm-PEG−PTH(1−34), Nterm-PEG−PTH(1−34), and the fitted curves by the model of the cylindrical core with Gaussian chains attached to the surface are shown in Figure 5. The aggregation number, N_{agg}, radius of gyration of the PEG chain in the corona, $R_{g\ PEG}$, the radius of the peptide core, R, and the length of the core, L, of the self-assembled core−shell structures are listed in Table 2.

As shown in Figure 5, there is a deviation of the fitted curves from all of the SANS profiles of monoPEGylated hPTH(1−34) at a high q region (q > 0.3 Å^{-1}). The scattering at a high q region is mainly originated from the polymer chains in the corona.[26] The Gaussian chain conformation assumed in this model does not take into account the excluded volume effect between monomers within the same polymer chain (self-avoidance), which is posed by real polymers.[34] Hence, when the local structure of the polymers is observed (higher q region), the Gaussian chain conformation cannot fully describe the real polymers. For monoPEGylated hPTH(1−34) at 55 °C, a deviation of the fitted curves from the SANS profiles at a low q region (q < 0.015 Å^{-1}) was also observed in Figure 5. This

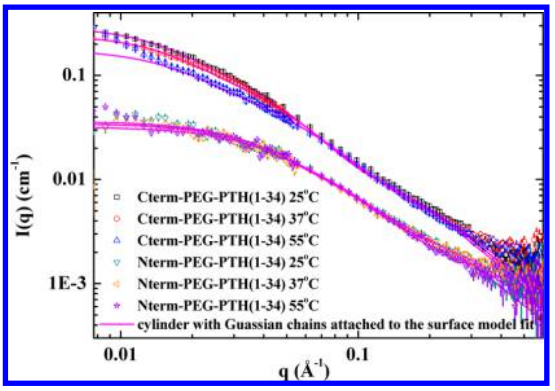

Figure 5. SANS profiles of Cterm-PEG−PTH(1−34) and Nterm-PEG−PTH(1−34) in phosphate buffer at (□) 25 °C, (○) 37 °C, and (△) 55 °C, and the curves are fitted by the model of the cylindrical core with Gaussian chains attached to the surface.

upturn at a lower q region reflects the attractive interactions between the cylindrical core−shell structures subjected to the elevated temperature.

Size Discrepancy of the Core−Shell Structures Because of Different PEGylation Sites. In Figure 5, there is a shift toward a lower q region for the scattering profiles of the Cterm-PEG−PTH(1−34) compared to the profile of Nterm-PEG−PTH(1−34). Moreover, the intensity at zero scattering angle of Cterm-PEG−PTH(1−34) is about 8 times higher than that of Nterm-PEG−PTH(1−34). These indicate that the self-assembled core−shell structure formed by Cterm-PEG−PTH(1−34) has a larger overall size. In addition, the aggregation number, N_{agg}, of the structure formed by Cterm-PEG−PTH(1−34) is larger than that of Nterm-PEG−PTH(1−34) ($N_{agg,Cterm}$ = 11, and $N_{agg,Nterm}$ = 3). The qualitative SANS profiles and quantitative model fitting data both demonstrate a size discrepancy between different PEGylation sites.

There are two interactions that dominant the interplay of the conjugated PEG chain and the peptide. First, the side chain of the cationic residues interacts favorably with the oxygen atoms on the PEG chains.[35−37] These favorable interactions make the conjugated PEG chain confine to the polar side of the peptide. Besides the charge−dipole interactions between the cationic residues and PEG, PEG also interacts with hydrophobic residues to reduce the surface-accessible solvent area of the peptide.[35]

The charge−dipole interactions and hydrophobic interactions between the peptide and the PEG chain affect the conformation of the conjugated PEG chain as well as the spatial arrangement of side chains of the residues in the peptide.[38] Different PEGylation sites could result in different hydrophobicity of the peptide part of the PEG−peptide conjugates. Because the hydrophobic region plays an important role in the process of self-assembly, the difference in hydrophobicity of the peptides, which is caused by different PEGylation sites, ultimately leads to a discrepancy in aggregation numbers. Therefore, we propose that the size variation between different PEGylation sites could be attributed to the collaborative contribution of charge−dipole interactions and hydrophobic interactions subjected to local residues and bonding.

Conformations of the Free PEG Chain and the Conjugated PEG Chain. Figure 6 shows the SANS profile of the free PEG chain in phosphate buffer, and the inset is the Guinier plot. The radius of gyration R_g of the free PEG chain calculated by the Guinier plot is 27 Å. The scattering intensity

dx.doi.org/10.1021/la501689d | Langmuir 2014, 30, 11421−11427

Table 2. Structural Parameters of the Core−Shell Structures Formed by Cterm-PEG−PTH(1−34) and Nterm-PEG−PTH(1−34) at 25, 37, and 55 °C

temperature (°C)	aggregation number, N_{agg}	radius of gyration of the PEG, $R_{g\ PEG}$ (Å)	core length, L (Å)	core radius, R (Å)
		Cterm-PEG−PTH(1−34)		
25	11	11.6 ± 0.1	255.5 ± 4.3	11.2
37	9	10.3 ± 0.1	245.0 ± 4.7	11.3
55	7	7.4 ± 0.1	240.0 ± 4.9	10.2
		Nterm-PEG−PTH(1−34)		
25	3	7.5 ± 0.3	103.9 ± 3.5	9.2
37	3	5.7 ± 0.3	95.1 ± 2.7	10.5
55	3	5.1 ± 0.3	104.5 ± 2.6	10.1

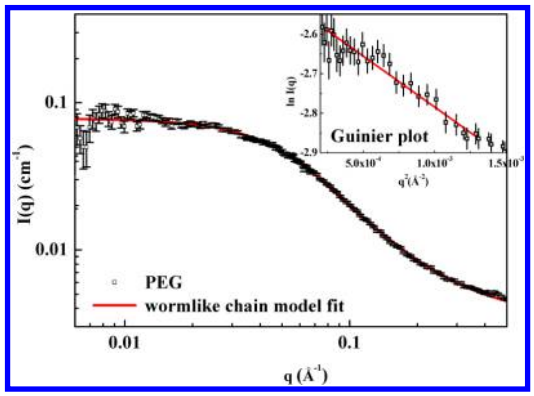

Figure 6. SANS profile of free PEG chain in phosphate buffer at 25 °C. The red curve represents the fit by the wormlike chain model. The inset shows the Guinier plot.

decays with approximately $I \sim q^{-1.65}$ at an intermediate q region, suggesting that the free PEG chain is swollen in phosphate buffer. Excluded volume effects between the monomers of the same polymer chain are responsible for the swelling of the polymer coil.[34] Hence, a wormlike chain model with an excluded volume effect is used to fit the SANS profile of the free PEG chain, as shown in Figure 6.

From the aforementioned model fittings, the radius of gyration of the conjugated PEG chain is smaller compared to that of the free PEG chain [R_g of the conjugated PEG = 11.6 and 7.5 Å for Cterm-PEG−PTH(1−34) and Nterm-PEG−PTH(1−34), respectively, and R_g of free PEG chain = 27 Å]. This suggests that the conjugated PEG chain either shrinks into a compressed polymer coil or collapses against the surface of the peptide core. Because the PEG part of the conjugates act as a protecting shell around the hydrophobic peptide core to reduce its solvent-accessible surface area, it is unlikely that PEG would shrink into a compressed polymer coil to expose the surface of the hydrophobic core. This leads us to discuss what favorable interactions between the conjugated PEG and the peptide can cause the PEG chain to collapse on the peptide core.

There are two interactions that dominant the interplay of the conjugated PEG chain and the peptide: charge−dipole interactions and hydrophobic interactions. The molecular dynamics simulation studies by Hamed et al.[35] and Jain et al.[36] both suggest that the charge−dipole interactions between the oxygen atoms on the PEG chain and the cationic residues are the most prominent interactions in PEG−peptide conjugates. Because there are several cationic residues in hPTH(1−34) under the condition of phosphate buffer (pH 7.4), a hypothetical description of our model fitting results is proposed as follows. When self-assembling into the core−shell structure, the side chain of the cationic residues near the PEGylation site would be prone to be located near the surface of the core to interact with the PEG chains. In comparison to the framework by Li et al.[39] for the core−shell structure with a hydration shell around the protein core surface, we illustrated Figure 7a. We show a detailed core−shell cylinder structure with the side chain of cationic residues located near the surface of the core. Moreover, according to the features yielded by our SANS model fitting, an abstract graphic illustration describes different levels of microstructures based on the spatial range of SANS. Thermodynamically, because of the charge−dipole interactions between the oxygen atoms on the PEG chain and cationic residues, the PEG chains bound to the surface of the peptide core (Figure 7b), which reduces the radius of gyration, instead of forming a compressed PEG coil (Figure 7c) or an unperturbed PEG coil (Figure 7d) adjacent to the peptide core.

CONCLUSION

In this study, we investigate hPTH(1−34) and monoPEGylated hPTH(1−34) at two different PEGylation sites in phosphate buffer from a structural point of view. The structure of

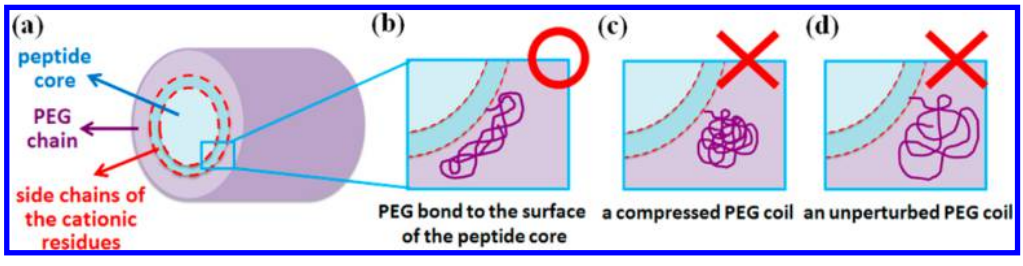

Figure 7. Schematic illustration of the (a) core−shell cylinder structure formed by monoPEGylated hPTH(1−34), (b) collapsed PEG chain on the surface of the peptide core, (c) compressed conformation, and (d) unperturbed conformation of the conjugated PEG chain. The cationic residues may locate near the surface of the peptide core to interact with the oxygen atoms on the PEG chain.

dx.doi.org/10.1021/la501689d | Langmuir 2014, 30, 11421−11427

hPTH(1−34) was found to undergo a dramatic change because of monoPEGylation. The particles of hPTH(1−34) aggregate into clusters in phosphate buffer because of hydrophobic effects. After monoPEGylation, the scattering contribution from the clusters disappeared. Instead, driven by the hydrophobic effect from the hydrophobic region of the peptide part of the conjugates, the units of monoPEGylated hPTH(1−34) self-assembled into a supermolecular core−shell cylinder structure. The PEG chains from different conjugates form a shell to shield the peptides from the solvent. With model fitting, quantitative structural information on monoPEGylated hPTH(1−34) revealed a more collapsed conformation of the conjugated PEG chain. We propose that the deformation of the PEG chain could be from the charge−dipole interactions between conjugated PEG and the peptide. The size of the core−shell structure formed by Cterm-PEG−PTH(1−34) was found to be 3 times larger than that of Nterm-PEG−PTH(1−34). Model fitting results suggested that the size discrepancy is from the difference in aggregation number because of different PEGylation sites, which could potentially affect the pharmacokinetics, such as circulating half-life, of the hPTH(1−34) drug for "biobetter" drug development.

■ ASSOCIATED CONTENT

Ⓢ Supporting Information

Surface structure of hPTH(1−34) visualized by the program PyMOL (Figure S1). This material is available free of charge via the Internet at http://pubs.acs.org.

■ AUTHOR INFORMATION

Corresponding Author

*E-mail: ewenhuang@nctu.edu.tw.

Notes

The authors declare no competing financial interest.

■ ACKNOWLEDGMENTS

The authors appreciate the advice of the editor and reviewers. The authors revised the manuscript accordingly. This work is supported by the Ministry of Science and Technology (MOST) of Taiwan (NSC-101-2221-E-008-039-MY3) and the Neutron Scattering User Proposals of the National Synchrotron Radiation Research Center (NSRRC) (N-2012-2-102-1 and N-2013-1-002). The authors greatly appreciate the SANS beam time from EQ-SANS of SNS and Bio-SANS of HFIR, ORNL. All of the authors appreciate the help by Dr. Changwoo Do and Dr. Chun-Jen Su for the SANS and small-angle X-ray scattering (SAXS) experiments, respectively.

■ REFERENCES

(1) Hwang, J. S.; Tu, S. T.; Yang, T. S.; Chen, J. F.; Wang, C. J.; Tsai, K. S. Teriparatide vs. calcitonin in the treatment of Asian postmenopausal women with established osteoporosis. *Osteoporosis Int.* **2006**, *17*, 373−378.

(2) Kung, A. W.; Pasion, E. G.; Sofiyan, M.; Lau, E. M.; Tay, B. K.; Lam, K. S.; Wilawan, K.; Ongphiphadhanakul, B.; Thiebaud, D. A comparison of teriparatide and calcitonin therapy in postmenopausal Asian women with osteoporosis: A 6-month study. *Curr. Med. Res. Opin.* **2006**, *22*, 929−937.

(3) Langdahl, B. L.; Rajzbaum, G.; Jakob, F.; Karras, D.; Ljunggren, O.; Lems, W. F.; Fahrleitner-Pammer, A.; Walsh, J. B.; Barker, C.; Kutahov, A.; Marin, F. Reduction in fracture rate and back pain and increased quality of life in postmenopausal women treated with teriparatide: 18-Month data from the European Forsteo Observational Study (EFOS). *Calcif. Tissue Int.* **2009**, *85*, 484−493.

(4) Quattrocchi, E.; Kourlas, H. Teriparatide: A review. *Clin. Ther.* **2004**, *26*, 841−854.

(5) Roberts, M.; Bentley, M.; Harris, J. Chemistry for peptide and protein pegylation. *Adv. Drug Delivery Rev.* **2002**, *54*, 459−476.

(6) Alconcel, S. N.; Baas, A. S.; Maynard, H. D. FDA-approved poly(ethylene glycol)−protein conjugate drugs. *Polym. Chem.* **2011**, *2*, 1442−1448.

(7) Carlsen, A.; Lecommandoux, S. Self-assembly of polypeptide-based block copolymer amphiphiles. *Curr. Opin. Colloid Interface Sci.* **2009**, *14*, 329−339.

(8) Harris, J. M.; Chess, R. B. Effect of pegylation on pharmaceuticals. *Nat. Rev. Drug Discovery* **2003**, *2*, 214−221.

(9) Harris, J. M.; Martin, N. E.; Modi, M. Pegylation: A novel process for modifying pharmacokinetics. *Clin. Pharmacokinet.* **2001**, *40*, 539−551.

(10) Veronese, F. M.; Pasut, G. Pegylation, successful approach to drug delivery. *Drug Discovery Today* **2005**, *10*, 1451−1458.

(11) Shu, J. Y.; Lund, R.; Xu, T. Solution structural characterization of coiled-coil peptide−polymer side-conjugates. *Biomacromolecules* **2012**, *13*, 1945−1955.

(12) Pai, S. S.; Hammouda, B.; Hong, K.; Pozzo, D. C.; Przybycien, T. M.; Tilton, R. D. The conformation of the poly(ethylene glycol) chain in mono-pegylated lysozyme and mono-pegylated human growth hormone. *Bioconjugate Chem.* **2011**, *22*, 2317−2323.

(13) Svergun, D. I.; Ekström, F.; Vandegriff, K. D.; Malavalli, A.; Baker, D. A.; Nilsson, C.; Winslow, R. M. Solution structure of poly(ethylene) glycol-conjugated hemoglobin revealed by small-angle X-ray scattering: Implications for a new oxygen therapeutic. *Biophys. J.* **2008**, *94*, 173−181.

(14) Shu, J. Y.; Tan, C.; DeGrado, W. F.; Xu, T. New design of helix bundle peptide−polymer conjugates. *Biomacromolecules* **2008**, *9*, 2111−2117.

(15) Lund, R.; Shu, J.; Xu, T. A small-angle X-ray scattering study of α-helical bundle-forming peptide−polymer conjugates in solution: Chain conformations. *Macromolecules* **2013**, *46*, 1625−1632.

(16) Guinier, A.; Fournet, G. *Small-Angle Scattering of X-rays*; Wiley: Hoboken, NJ, 1955.

(17) Roe, R.-J. *Methods of X-ray and Neutron Scattering in Polymer Science*; Oxford University Press: New York, 2000; Vol. *130*.

(18) Kline, S. Reduction and analysis of SANS and USANS data using IGOR Pro. *J. Appl. Crystallogr.* **2006**, *39*, 895−900.

(19) Kohlbrecher, J. *SASfit, 3*; Laboratory for Neutron Scattering, Paul Scherrer Institute (PSI): Villigen, Switzerland, 2006.

(20) Rai, D. K.; Beaucage, G.; Jonah, E. O.; Britton, D. T.; Sukumaran, S.; Chopra, S.; Gonfa, G. G.; Härting, M. Quantitative investigations of aggregate systems. *J. Chem. Phys.* **2012**, *137*, 044311−044316.

(21) Marx, U. C.; Adermann, K.; Bayer, P.; Forssmann, W. G.; Rosch, P. Solution structures of human parathyroid hormone fragments hPTH(1−34) and hPTH(1−39) and bovine parathyroid hormone fragment bPTH(1−37). *Biochem. Biophys. Res. Commun.* **2000**, *267*, 213−220.

(22) Schrödinger, LLC. *The Pymol Molecular Graphics System, 1.3r1*; Schrödinger, LLC: New York, 2010.

(23) Fink, H. P. Structure analysis by small-angle X-ray and neutron scattering. *Acta Polym.* **1989**, *40*, 224−224.

(24) Beaucage, G. Approximations leading to a unified exponential/power-law approach to small-angle scattering. *J. Appl. Crystallogr.* **1995**, *28*, 717−728.

(25) Kamberi, M.; Chung, P.; DeVas, R.; Li, L.; Li, Z.; Ma, X. S.; Fields, S.; Riley, C. M. Analysis of non-covalent aggregation of synthetic hPTH(1−34) by size-exclusion chromatography and the importance of suppression of non-specific interactions for a precise quantitation. *J. Chromatogr. B: Anal. Technol. Biomed. Life Sci.* **2004**, *810*, 151−155.

(26) Pedersen, J. Form factors of block copolymer micelles with spherical, ellipsoidal and cylindrical cores. *J. Appl. Crystallogr.* **2000**, *33*, 637−640.

(27) Pedersen, J. S.; Gerstenberg, M. C. Scattering form factor of block copolymer micelles. *Macromolecules* **1996**, *29*, 1363−1365.
(28) Förster, S.; Burger, C. Scattering functions of polymeric core−shell structures and excluded volume chains. *Macromolecules* **1998**, *31*, 879−891.
(29) Liu, Y.; Chen, S.-H.; Huang, J. S. Small-angle neutron scattering analysis of the structure and interaction of triblock copolymer micelles in aqueous solution. *Macromolecules* **1998**, *31*, 2236−2244.
(30) Livsey, I. Neutron scattering from concentric cylinders. Intraparticle interference function and radius of gyration. *J. Chem. Soc., Faraday Trans. 2* **1987**, *83*, 1445−1452.
(31) Fournet, G. Scattering functions for geometrical forms. *Bull. Soc. Fr. Mineral. Cristallogr.* **1951**, *74*, 75.
(32) Debye, P. Molecular-weight determination by light scattering. *J. Phys. Colloid Chem.* **1947**, *51*, 18−32.
(33) Strickland, L. A.; Bozzato, R. P.; Kronis, K. A. Structure of human parathyroid hormone(1−34) in the presence of solvents and micelles. *Biochemistry* **1993**, *32*, 6050−6057.
(34) Lindner, P.; Zemb, T. *Neutrons, X-rays, and Light: Scattering Methods Applied to Soft Condensed Matter*; Elsevier: Amsterdam, Netherlands, 2002.
(35) Hamed, E.; Xu, T.; Keten, S. Poly(ethylene glycol) conjugation stabilizes the secondary structure of α-helices by reducing peptide solvent accessible surface area. *Biomacromolecules* **2013**, *14*, 4053−4060.
(36) Jain, A.; Ashbaugh, H. S. Helix stabilization of poly(ethylene glycol)−peptide conjugates. *Biomacromolecules* **2011**, *12*, 2729−2734.
(37) Xue, Y.; O'Mara, M. L.; Surawski, P. P.; Trau, M.; Mark, A. E. Effect of poly(ethylene glycol) (PEG) spacers on the conformational properties of small peptides: A molecular dynamics study. *Langmuir* **2011**, *27*, 296−303.
(38) Hamley, I. W.; Ansari, I. A.; Castelletto, V.; Nuhn, H.; Rosler, A.; Klok, H. A. Solution self-assembly of hybrid block copolymers containing poly(ethylene glycol) and amphiphilic β-strand peptide sequences. *Biomacromolecules* **2005**, *6*, 1310−1315.
(39) Li, D.; Hu, T.; Manjula, B. N.; Acharya, S. A. Non-conservative surface decoration of hemoglobin: Influence of neutralization of positive charges at pegylation sites on molecular and functional properties of pegylated hemoglobin. *Biochim. Biophys. Acta, Proteins Proteomics* **2008**, *1784*, 1395−1401.
(40) Gronwald, W.; Schomburg, D.; Tegge, W.; Wray, V. Assessment by ^{1}H NMR spectroscopy of the structural behaviour of human parathyroid-hormone-related protein(1−34) and its close relationship with the N-terminal fragments of human parathyroid hormone in solution. *Biol. Chem.* **1997**, *378*, 1501−1508.